IL NUOVO CIMENTO **41 C** (2018) 119
DOI 10.1393/ncc/i2018-18119-3

COMMUNICATIONS: SIF Congress 2017

The fast neutron and proton irradiation facility at the INFN Legnaro National Laboratory

L. SILVESTRIN([1])([2])

([1]) *Dipartimento di Fisica, Università di Padova - Padova, Italy*
([2]) *INFN, Sezione di Padova - Padova, Italy*

received 31 January 2018

Summary. — The availability at the INFN Legnaro National Laboratory of two new accelerator systems, the 70 MeV cyclotron of the SPES project and the 5 MeV RFQ developed for the TRASCO project, makes it possible to build a suite of neutron sources for a wide spectrum of different applications. This article focuses on the facility at the SPES cyclotron (NEPIR), which is in an advanced design phase. NEPIR will deliver quasi mono-energetic neutrons for multi-disciplinary applications and a complementary fast ($E_{\mathrm{n}} > 1\,\mathrm{MeV}$) neutron field with a continuous energy (atmospheric-like) spectrum for studying neutron-induced effects on materials, *e.g.*, single event effects in electronics.

1. – Introduction

At the Legnaro National Laboratories (LNL, Italy) a large program is under way to create a suite of accelerators and neutron production targets for a wide range of research and applications consisting of the Legnaro Slow Neutron Source (LSNS) and NEPIR (Neutron and Proton IRradiation facility) at the SPES complex [1].

LSNS will be driven by a 30–40 mA, 5 MeV proton RFQ with Li and Be targets. The LSNS project encompasses cross-disciplinary R&D using cold, thermal, epithermal and fast (up to 5 MeV) neutrons to serve users from academia, government laboratories, and industries in Italy, Europe and beyond, in a variety of research programs. The new SPES high current (0.75 mA), 70 MeV proton cyclotron will drive NEPIR: a fast neutron irradiation multipurpose facility, originally conceived to study the Single Event Effects (SEE) induced by neutrons and protons in microelectronic devices.

While the LSNS system is a long term goal, in this work we will focus exclusively on the NEPIR project as it is in an advanced design phase, is partially funded and the construction of the bunker will soon begin. NEPIR is based on two different neutron production targets in order to generate high flux neutron beams with different energy spectra: a quasi mono-energetic beam and a complementary white spectrum beam with energy distribution similar to that of neutrons naturally present at sea-level (atmospheric neutrons), generated by the interaction of energetic cosmic rays with the Earth atmosphere.

2. – The neutron and proton irradiation facility

NEPIR is an irradiation facility that will use the high current ($750\,\mu$A) proton cyclotron of the SPES project, energy tunable in the 35–70 MeV interval, to alternatively feed two different neutron converters. The first will produce a Quasi Mono-energetic Neutron beam (QMN), with controllable energy peak in the 20–70 MeV range; this versatile tool will be an important addition to the park of research infrastructures for National and European research. The second converter will produce fast ($E_{\mathrm{n}} > 1\,\mathrm{MeV}$) neutrons with an energy distribution similar to that of atmospheric neutrons. In this neutron source, additional moderator panels can be used to further shape the white spectrum to resemble that of other environments (*e.g.*, surface of Mars). The maximum proton current available at NEPIR will be limited to $10\,\mu$A for radioprotection reasons; the minimum proton beam energy will be decreased down to 20 MeV by means of a carbon energy degrader system.

3. – QMN

Quasi Mono-energetic Neutron reference fields can be used to study energy dependent neutron interaction mechanisms with matter, be it electronic, detector, dosimeter material, or living tissues [2-4]. Such a tool is used in diverse research fields for many applications:

- neutron effects in electronics (space-craft, avionics and state-of-the-art, or high reliability systems at sea-level . . .);
- detectors R&D (response and calibration of neutron detectors, but also of detectors for different applications, such as medicine, dark matter experiments . . .);
- nuclear physics (cross-section data for basic science, Monte Carlo codes development, research on transmutation of radioactive waste . . .);
- medical and radiation protection applications (shielding-benchmark experiments, effects of secondary neutrons on patients, on accelerators facility personnel or ancillary electronics . . .).

Energetic QMN fields are commonly produced exploiting the reactions ^{7}Li(p,xn) and ^{9}Be(p,xn) using thin (few mm) Li or Be targets that do not stop the proton beam; the emerging protons are then magnetically deflected towards a beam dump. The resulting neutron energy spectrum in the forward direction (fig. 1, left) is not purely mono-energetic: it does present a high energy peak few MeV below the energy of the impinging protons, but also a broad distribution at lower energy (tail), coming from nuclear breakup [5, 6] that accounts for roughly a half of the total energetic neutron production. This continuous energy tail changes little with emission angle, while the fraction of neutrons in the mono-energy peak decreases rapidly with angle. This behavior can be exploited to correct data taken in the forward direction, by subtracting the effect due to neutrons in the wrong-energy tail, that can be measured taking data also at larger angles (usually in the $15°$–$30°$ range) (fig. 1, right) [7].

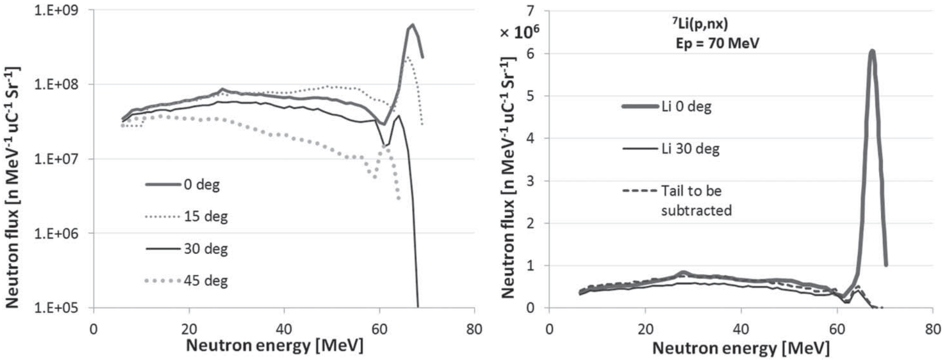

Fig. 1. – (Left) double differential neutron yield, as a function of neutron energy and emission angle, generated by a 70 MeV proton beam impinging on a 4.7 mm thick Li target. (Right) correction of quasi-monochromatic forward Li spectrum using 30° data (impinging proton beam energy: 70 MeV) [7].

The optimal angle for data correction, for energies below 70 MeV, will be experimentally determined: in this energy range, very few data are available in the literature and Monte Carlo calculations are not entirely reliable.

The width of the mono-energetic peaks comes from two contributing factors: the existence of excited states of Li and Be that can be reached in the ^{7}Li(p,n) and ^{9}Be(p,n) reactions at the proton beam energies available at NEPIR and the energy loss of the primary beam propagating along the target thickness. The latter is a controllable parameter: if the target thickness decreases the peak width will also decrease, but at the price of a lower neutron yield. For low power deposition, Li targets perform better than Be ones, providing both a sharper mono-energetic peak and higher yield. At high power Be is favored because of its better thermal and mechanical properties.

The QMN source of the NEPIR facility will use different proton beam energies and an assortment of thin Li targets, 1 to 4 mm thick, as a function of the required peak width, to produce nearly mono-energetic neutrons at several discrete energies. A multi-angle collimator system will allow wrong-energy tail effect corrections as well as measurements of the angular dependence of nuclear cross-sections of different materials.

To allow neutron peak energy below the minimum energy cutoff (35 MeV) of the cyclotron, a carbon energy degrader will be used to decrease the primary proton beam energy down to 20 MeV. The energy degrader will be located upstream in the cyclotron hall to minimize neutron contamination in the NEPIR area. The current loss due to the degradation can be at least partially compensated increasing the current extracted from the cyclotron, the constraints being the radioprotection regulations.

The QMN source at NEPIR is expected to provide a maximum flux of mono-energetic neutrons (in the peak energy interval) $\sim 3 \times 10^5$ n cm^{-2} s^{-1} at a test point at a distance $d = 3$ m, for $I = 10\,\mu$A and proton energy 70 MeV.

4. – ANEM

ANEM is a neutron source specifically tailored to study the effects of atmospheric neutrons on material, in particular electronic devices and systems at sea level, but also at flight altitudes (avionics) where the neutron flux is 300–450 times higher.

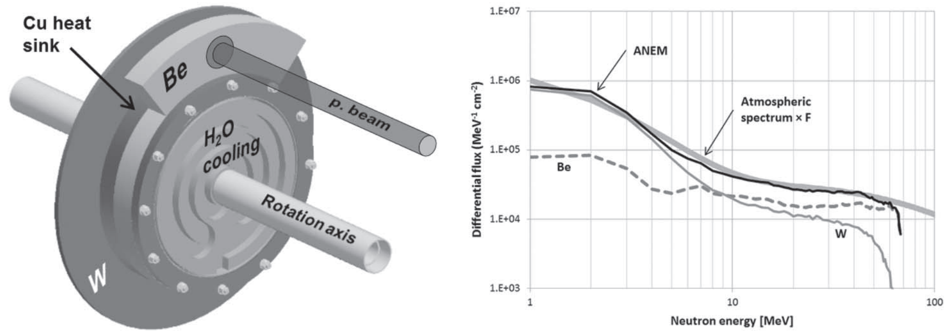

Fig. 2. – (Left) the 32 cm diameter Be and W circular sectors of ANEM intercept the 13 cm off-axis proton beam; the stainless steel rotating drum (diameter 18 cm) houses the helicoidal water cooling circuit. (Right) the ANEM neutron spectrum (black line) with 70 MeV protons and 10 μA current at a distance 3 m downstream, compared to the reference sea-level one (thick grey line) multiplied by an acceleration factor $F = 3\times10^9$. The ANEM spectrum is the weighted sum of the spectra of the two sectors: Be 21%, W 79%.

The ANEM source is designed to generate an atmospheric-like neutron spectrum using a rotating composite target composed by a Be sector followed by a coaxial W disk (fig. 2, left). The 70 MeV proton beam is off axis and it alternatively strikes the Be (21% of the time) and then the W, so that the proton beam energy is deposited over a large area. The W disk is 5 mm thick to stop the 70 MeV protons; on the other hand the Be is 24 mm thick, not enough to stop the protons to avoid blistering due to hydrogen build in the Be. The spent protons emerging from the Be are then stopped in the W.

Monolithic coaxial Cu rings (fig. 2, left) are used for mechanical and thermal coupling to the rotating steel drum cooled by a helicoidal water system. This design was simulated using finite elements calculations (ANSYS code) to assess the thermo-mechanical properties of the target. Assuming a proton beam spot with a Gaussian distribution (1 cm FWHM), the power safety limit of the target was calculated to be 3.5 kW, using a 0.2 l/s cooling water flux at a temperature of 10 °C and a 2 Hz target rotation frequency. This corresponds to a maximum current of 50 μA, well above the maximum available at NEPIR. In terms of thermal-mechanical performance, the Be sector is less problematic because of the lower amount of deposited energy and the higher thickness of the material that contributes to a better power dissipation.

The W(p,xn) reaction is used to generate neutrons which well reproduce the sea level neutron spectrum up to ∼50 MeV, at a higher energy the yield decreases too rapidly (fig. 2, right). The light Be is used to adjust the neutron yield in this interval and extend the pseudo-atmospheric spectrum up to ∼65 MeV.

Monte Carlo simulations were used to calculate the optimal Be fraction (21%) to model the atmospheric neutron spectrum in the fast neutrons region. The calculated fast neutron flux, at a test point 3 m downstream, at the maximum proton current available at the facility (10 μA) is 10^7 n cm^{-2} s^{-1}, corresponding to an acceleration factor $F = 3\times10^9$ (*i.e.*, the flux is F times higher than the natural one).

As mentioned above, Monte Carlo calculations of the neutron production from Be are not entirely reliable in this energy range. Before the design of ANEM can be validated, measurements of the neutron spectrum from a thick Be target are required.

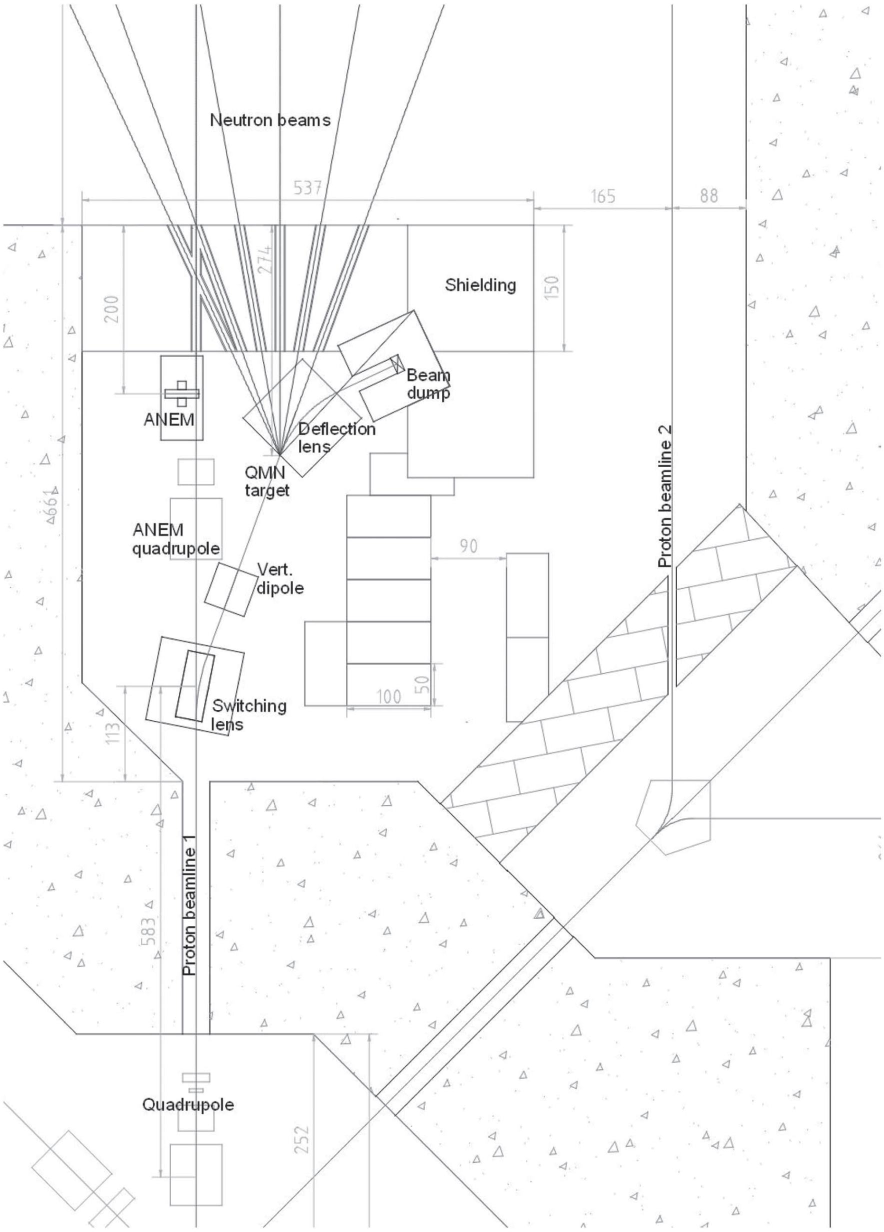

Fig. 3. – Schematic drawing of the floor plan of the NEPIR irradiation facility indicating position and overall dimensions (units in cm) of the different elements of the facility. The proton beam comes from the bottom, passing through the switching lens towards the ANEM system, or the QMN source. The dashed lines show the different neutron beamlines departing from the QMN source in different directions (0° to 45°) and form the ANEM system in the forward direction. A shielding configuration is shown, made up of concrete blocks, 150 cm thick, with an access maze visible on the right.

Alternative and cheaper designs of the ANEM source are also under study. To significantly decrease the cost, and to better withstand thermal-mechanical stress, the W disk can be divided into many small separate blades. The neutron spectrum generated by the W alone can then be shaped, by using a 3 cm thick borated polyethylene moderator, to acceptably resemble the atmospheric one, but at the price of a 50% decrease of the acceleration factor. Finally, thin W targets ($\sim$1 mm) can be used in the QMN system to generate a low flux pseudo-atmospheric neutron spectrum.

5. – Facility layout

The present design of the layout of NEPIR is shown in fig. 3: the proton beam comes from the cyclotron hall (bottom of the figure) where focusing quadrupoles are located. The ANEM target and the QMN target are located in a heavily shielded bunker made up of 150 cm thick concrete walls and ceiling. As the proton beam enters the bunker it passes through the switching magnet that selects the target systems.

The ANEM target is installed on the extension of the beamline coming from the cyclotron hall; in this position a direct line of sight can be created from the test point to the cyclotron exit. For this reason, we expect a small ($\ll$1%) contamination of the fast neutron atmospheric spectrum at the test point by neutrons and gammas coming from the beam losses in the beam extraction and transport from the cyclotron hall. The limited current (10 μA max) of the NEPIR facility and the distance of the ANEM target from the bunker beamline entrance limit the dose rate by neutrons backstreaming towards the cyclotron hall below 100 μSv/h, less than 1/10th of the dose level generated by the cyclotron alone. The long distance separating ANEM from the quadrupoles (bottom of fig. 3) in the cyclotron hall requires a set of two more dipoles to properly focus the proton beam on the target.

Energizing the switching magnet, the proton beam is deviated towards the QMN system (20° from ANEM direction) where it passes through the thin Li target and is deflected (45°) towards the heavily shielded beam dump. A set of 10 cm diameter iron collimators shapes the neutron beams towards the experimental hall; during normal operation all the collimators, except one, will be closed by an iron rod, to minimize the dose in the experimental hall. The collimated neutron beams propagate through the experimental hall up to a concrete neutron absorber (not shown in fig. 3) located on the other side of the hall, 6.5 m downstream of the bunker shielding. The limited fraction of the air of the experimental hall directly exposed to the neutron beam avoids excessive air activation (<1 Bq/g after a 24 h long irradiation at full 10 μA current). On the contrary, the activation level of the air inside the bunker (<60 m^3) will quickly exceed the radioprotection regulation limit of 1 Bq/g. For this reason, the bunker is airtight (the access maze is closed by a door and the collimator apertures by a thin Al slab), kept at a pressure slightly lower than the outside one, to avoid any leakage, and vented with 2 air changes per hour to limit activation. The air extracted from the bunker is managed and exhausted by the air collection system of the SPES building through a central chimney equipped with activity monitoring.

6. – Conclusions

The design of the NEPIR facility is in an advanced phase and the construction of the bunker should begin in 2019. The QMN system is the main tool and will be constructed in two phases: a first, very low current ($\ll$1 μA) test phase in which the neutron spectra from thin Li targets at various energies and angles will be measured in order to finalize the design of the multi-collimator system. In addition the spectrum of a thick Be target will be measured, to validate the design of the ANEM system. The installation of the ancillary activated air management system and the realization of the definitive multi-angle collimator will allow to upgrade to full current (phase 2) and to complete and install the ANEM converter.

The final relevant tool will be a low current direct proton beam irradiation chamber to be initially installed at the 0° test position of the QMN system; in the future it should be moved to a dedicated beam line (beamline 2 in fig. 3).

REFERENCES

[1] Bisello D. *et al.*, *J. Phys. Conf. Ser.*, **1021** (2018) 012010.
[2] Pomp S. *et al.*, *High-energy quasi-monoenergetic neutron fields: existing facilities and future needs*, EURADOS Report 2013-02, Braunschweig, May 2013.
[3] Harano H. and Nolte R., *Metrologia*, **48** (2011) S292.
[4] Nolte R. *et al.*, *Nucl. Instrum. Methods A*, **476** (2002) 369.
[5] Satoh D. *et al.*, *J. Nucl. Sci. Technol.*, **2** (2002) 657.
[6] Baba M. *et al.*, *Nucl. Instrum. Methods A*, **428** (1999) 454.
[7] Kamada S. *et al.*, *J. Korean Phys. Soc.*, **59** (2011) 1676.